EUROPEAN FUSION DEVELOPMENT AGREEMENT
JET

EFDA–JET–CP(06)03-15

R. Guirlet, C. Angioni, C. Bourdelle, L. Carraro, N. Dubuit,
R. Dux, X. Garbet, C. Giroud, G.T. Hoang, V. Naulin,
T. Parisot, M.E. Puiatti, P. Strand, P.R. Thomas, H. Weisen, K.D. Zastrow
and JET-EFDA Contributors

Parametric Dependences of Impurity Transport in Tokamaks

Parametric Dependences of Impurity Transport in Tokamaks

R. Guirlet[1], C. Angioni[2], C. Bourdelle[1], L. Carraro[3], N. Dubuit[1],
R. Dux[4], X. Garbet[1], C. Giroud[5], G.T. Hoang[1], V. Naulin[6],
T. Parisot[1], M.E. Puiatti[3], P. Strand[7], P.R. Thomas[1], H. Weisen[7], K.D. Zastrow[5]
and JET-EFDA Contributors*

Fusion Energy 2000 (Proc. 18th Int. Conf. Sorrento, 2000), IAEA, Vienna (2001).

Preprint of Paper to be submitted for publication in Proceedings of the
33rd EPS Conference,
(Rome, Italy 19-23 June 2006)

ABSTRACT

The neoclassical and turbulent models for impurity transport are reviewed. Analytical expressions of the neoclassical terms and the role of the impurity collisionality are summarised. A global presentation of the turbulence models for impurity transport is made. An quasi-linear fluid expression of the turbulent impurity flux is discussed. Theoretical and experimental aspects of the relative contributions of the neoclassical effects and of the turbulent effects are presented. The convective term of the flux is shown to depend largely on the main ion density and temperature gradients and on the dominant turbulent modes. Finally the dependence of the impurity flux on the impurity charge is reviewed. It is shown that both neoclassical and turbulent diffusion coefficients are predicted to decrease with increasing charge, while the neoclassical temperature screening effect increases with Z.

1. INTRODUCTION

For many years impurity transport in tokamaks and other fusion devices has puzzled experimentalists and theoreticians. Until recently, only the effect of collisions between different particle species had been theorised (under the name of neoclassical theory). The neoclassical predictions were far from the early experimental observations, performed in ohmic or degraded (L-mode) confinement regimes. The difference was attributed to the effect of turbulence but no theoretical model was available. With the development of so-called improved confinement regimes such as the H mode and its likes, and later the internal transport barrier (ITB) regimes, the global picture of impurity transport became even more complex. In some experiments the observations were closer to the neoclassical predictions but the same improved confinement regime could produce different results in different machines. Recently, a number of theoretical models for turbulent impurity transport have been developed, converging toward a coherent description of the phenomenon and thus giving rise to dedicated experiments. The encouraging results and the prospective of a complete impurity transport theory has given renewed incentive for a more systematic approach of the subject by comparing the predicted and observed dependences of the transport phenomenon on physical quantities. This paper aims at summarising the predictions of both theories and the recent comparisons with experimental results. Sections 2 and 3 are dedicated to the salient features of the neoclassical and turbulence theories respectively. Only the core of the theories will be reviewed, the situations at the margin of the theories (such as steep pedestals where the impurity Larmor radius is larger than the gradient lengths, or the effect of the wide banana orbits near the plasma centre) will not be discussed. In the discussion the assumption of negative density and temperature gradients is made everywhere in the plasma. This assumption will be recalled when necessary. Section 4 examines three particularly important questions present throughout the published studies, namely the relative contributions of collisions and of turbulence in the observed impurity transport, the direction of the impurity convective flux and the impurity charge dependence of the transport coefficients. For each of these questions, theoretical expectations are presented and the recent experimental results are reported.

NB: All physical quantities are expressed in SI units, including those derived from publications using cgs units.

2. NEOCLASSICAL THEORY

2.1 NEOCLASSICAL FLUX EXPRESSION

The neoclassical theory describes the contribution of collisions between different species to the radial transport of particles and heat in a plasma of tokamak-type geometry. As far as impurities are concerned, it has been developed mainly in the ‘70s [1, 2, 3, 4, 5, 6] and described ab initio in a most complete review by Hirshman and Sigmar in 1981 [7]. Since then, a few publications have been dedicated to providing i) approximate analytical expressions [8, 9] and ii) exact numerical values of the impurity particle fluxes [10, 11].

A few hypotheses are made throughout most of the theoretical literature. The small aspect ratio (the ratio of the plasma minor radius to its major radius) hypothesis, for example, has to be made if analytical flux expressions are to be obtained. It has to be noticed however that NCLASS does not use this hypothesis. Other hypotheses are made, such as the small Larmor radius and the small ion to impurity mass ratio.

Since in all tokamaks the collisions between any ion species and electrons are much less frequent than collisions between different ion species, the neoclassical electron flux is always neglected in the literature, which leads to a specific form of the ambipolarity constrain (which is itself an expression of the momentum conservation):

$$\Gamma_D + \sum_Z Z\Gamma_Z = 0 \tag{1}$$

where Γ_D is the main ion (generally deuterium) flux and the sum concerns every ionisation stage of every other ion species.

The theory of collisional transport, or neoclassical theory, acknowledges the existence of three terms. First, a term arises from collisions due to species gyrating around their guiding-centre with their Larmor radius. The second term takes into account further excursions specific to the tokamak situation. The third term corresponds to detrapping collisions of banana particles. A fourth term called electrostatic trapping term and explicited in [7] (eq. 3.23 and p. 1099) is estimated potentially to play a role for heavy impurities. It will not be discussed here.

Each term is described in the following paragraphs with the assumption of only one impurity species present in the plasma. Although this is never the case in the experiments, it is a good approximation as long as the friction force of the additional impurity species on the considered impurity species remains small compared to that of the working ion species. Corrections to be made in the case of multiple species are discussed in §2.1.5.

The flux expressions and their interpretation are taken from the fundamental review in [7] and the more practical developments of [8] which contains also a few corrections to the former.

2.1.1 Classical Flux

The classical flux is the consequence of the perpendicular friction force due to collisions between ions whose excursions around their guiding-centres are of the order of their Larmor radius. This flux term is present in a plasma of cylindrical geometry. The classical flux is expressed as the sum of a diffusive term and a convective

term [8]:

$$\Gamma^{cl}_{Z} = -D^{cl}_{Z}\left[\nabla_{nZ} - \frac{\upsilon^{cl}_{Z}}{D^{cl}_{Z}} n_Z \right] \tag{2}$$

where

$$D^{cl}_{Z} = \frac{8\sqrt{\pi}}{3} \frac{e^2 ln\Lambda_{DZ}}{(4\pi\varepsilon_0)^2 B^2} \sqrt{\frac{m_D}{2kT_i}} \frac{n_D}{Z_D} \tag{3}$$

and

$$\frac{\upsilon^{cl}_{Z}}{D^{cl}_{Z}} = \frac{Z}{Z_D} \left[\frac{\nabla n_D}{n_D} - \left(\frac{1}{2} + \frac{Z_D}{Z} \right) \frac{\nabla T_i}{T_i} \right] \tag{4}$$

In these expressions e is the elementary charge, ln Λ_{DZ} is the Coulomb logarithm for D-impurity collisions, B is the toroidal magnetic field, m_D and n_D are the deuterium mass and density respectively and T_i is the ion temperature (assumed to be the same for all ion species). The sign convention is such that v > 0 corresponds to an outward flux. It can be seen from eq. (4) that the main ion density gradient and the ion temperature gradient, both monotonously negative in most cases, will be responsible for opposite convective fluxes: the $\nabla n_D/n_D$ term will be directed inward while the $\nabla T_i/T_i$ term will be directed outward. This effect is the first indication of the so called 'temperature screening' which will be discussed in more detail along the next paragraphs. As Z increases the latter term tends to balance the former if $\nabla T_i/T_i = 2\nabla n_D/n_D$. More generally, the effectiveness of the temperature screening effect will increase with the ratio of the temperature to density normalised gradients.

The impurity diffusion coefficient given above is almost independent of the impurity species (the Coulomb logarithm is a weak function of the species). This is true when only one impurity species is present in the plasma. In the more realistic cases in which more than one species is present, one has to take into account collisions between the various impurity species, which add new terms in the classical flux (as well as in the other terms).

2.1.2 Pfirsch-Schlüter Flux

The Pfirsch-Schlüter flux results from the poloidal variation of the parallel friction forces due to pressure and temperature variations within a magnetic surface. It is the dominant flux term in the short mean free path regime (see discussion in 2.1.4). It is given by [8]:

$$\Gamma_Z^{PS} = -D_Z^{PS}\left[\nabla n_Z - \frac{\upsilon_Z^{PS}}{D_Z^{PS}} n_Z \right] \tag{5}$$

where

$$D_Z^{PS} = 2q^2 K D_Z^{cl} \tag{6}$$

and

$$\frac{v_Z^{PS}}{D_Z^{PS}} = \frac{Z}{Z_D} \left(\frac{\nabla n_D}{n_D} + \frac{H}{K} \frac{\nabla T}{T} \right) \tag{7}$$

with q the safety factor and H and K being functions of the impurity strength parameter $\alpha_Z = n_Z Z^2/n_D Z^2_D$ and of the main ion collisionality ν^*_D:

$$H = -\frac{1}{2} + \frac{0.29 + 0.68\alpha}{0.59 + a + 1.34(\in^{3/2}\nu^*_D)^{-2}} \tag{8}$$

$$H = 1 - \frac{0.52\alpha}{0.59 + a + 1.34(\in^{3/2}\nu^*_D)^{-2}} \tag{9}$$

It can be seen from eq.9 that K is never far from unity (because $\nu^*_D << 1$ in most present day experiments and a fortiori in ITER), which means that the Pfirsch-Schlüter diffusion coefficient is close to the classical one except at the edge where q can approach 10 in some experimental situations.

Unlike the classical flux, the second term of the convective flux can in principle be in either direction depending on α and ν^*_D. In ITER, assuming a deuterium collisionality $\nu^*_D \simeq 0.06$ in the plasma core, the coefficient H/K is anticipated to be -1/2, independently of α. The Pfirsch-Schlüter temperature gradient term will thus be directed outward (if $\nabla T_i/T_i < 0$) and will counteract partly the main ion density term, as in the classical flux. Until recently a at density gradient was expected over most of the plasma minor radius of the ITER reference scenario (H mode). This could lead to a net decontaminating effect. However, an anomalous inward pinch such as observed recently in several tokamaks [35, 36, 37] could result in a peaked main ion density profile and thus to a weaker decontaminating effect or even to a net inward impurity convective flux. The impurity density profiles could thus be more peaked than the main ion density profile, a phenomenon known as impurity accumulation. As an example, the density gradient and the temperature gradient terms have been calculated for a Tore Supra discharge in which the density profile peaking ($n_e(0)/<n_e>\simeq 1.7$) is controlled entirely by the anomalous pinch [35]. Fig.1 shows these two terms and their sum calculated for a typical carbon concentration of 3% (carbon is the main intrinsic impurity in Tore Supra). The total neoclassical convective flux is discussed in more detail in 4.2.

2.1.3 Banana-plateau Flux

The banana-plateau flux is driven by the surface averaged pressure tensor anisotropies and is dominant in the long mean free path regime. As the former two it can be expressed as [8]:

$$\Gamma_Z^{BP} = -D_Z^{BP} \left[\nabla n_Z - \frac{v_Z^{BP}}{D_Z^{BP}} \right] \tag{10}$$

where
$$D_Z^{BP} = \frac{3}{2} \frac{kT_i A_Z^{BP}}{Z^2 e^2 B^2_\psi R^2_{nZ}} \tag{11}$$

and
$$\frac{\nu_z^{BP}}{D_Z^{BP}} = \frac{Z}{Z_D} \frac{\nabla n_D}{n_D} + \alpha_{T_D}^{BP} \frac{\nabla T_i}{T_i} \tag{12}$$

The parameter αT_D^{BP} is given by:

$$\alpha_{T_D}^{BP} = \frac{3}{2}\left(1 - \frac{Z}{Z_D}\right) + \left(\frac{Z}{Z_D} \frac{K_{12}^D}{K_{11}^D} - \frac{K_{12}^D}{K_{11}^D}\right) \tag{13}$$

and the A^{BP}_Z and K^a_{ij} coefficients are functions of the impurity related quantities Z, m_Z, n_Z. They can be calculated from Appendix A of [8], replacing mistyped expressions (A.17-18) with expressions (4.63-64) of [7]. Here again the screening effect can play a role, although the complex dependences of αT_D^{BP} does not allow a straightforward evaluation.

2.1.4 Dominant Flux and collisional regime

Depending on the collisional regime, i.e. on the type of trajectories contributing to diffusion, one or another of the above fluxes will dominate the total flux of a given impurity species. Several publications have been devoted to specific experimental situations: main ion and impurity in the banana or plateau regime [1, 2]; main ion in banana regime and impurity in Pfirsch-Schlüter regime [3, 5]; main ion and impurity in Pfirsch-Schlüter regime [4, 6]. However the starting equations and the development formulation vary from one publication to another and it is not straightforward to extract the practical information. The relative contribution of the terms explicited in the previous paragraphs is discussed in [8] for TEXT and Alcator-C experiments and in [11] for ASDEX-U H-mode experiments. As an example, the neoclassical flux expressions given above have been applied to a Tore Supra deuterium plasma in which a laser blow-off injection of nickel was performed. Fig.2(a) shows that the nickel ions are deep in the high collisionality regime over the whole plasma while Figs.2(b) and 2(c) evidence the non-negligible contribution of the classical and banana-plateau uxes. Conversely, Fig.2(d) shows that, although the intrinsic carbon ions are in the banana-plateau regime, the Pfirsch-Schlûter flux plays a substantial role in both transport coefficients.

2.1.5 The multi-species case

The analytical expressions given above assume the presence of only one impurity species mixed with the main ion species. A more realistic description of present day experiments should contain several impurity species. In the TFTR [43] and JET [12] D-T experiment cases and in the D-T ITER operating phase, the description must even contain two main ion species, D and T. In TEXTOR-94 the tungsten ion collisions on neon are shown to be responsible for a neoclassical inward convective flux which governs the central W accumulation [13]. Only by controlling the neon concentration (either the gas pu or the edge plasma recycling conditions) can this flux be kept to a level low enough not to provoke central accumulation.

3. TURBULENCE THEORY

3.1 THEORETICAL MODELS FOR THE IMPURITY TURBULENT FLUX

Despite the evidence of non-neoclassical transport in many experimental situations, models of the impurity transport caused by electrostatic turbulence have been developed only recently (the magnetic turbulence is thought to play a minor role in transport). The theoreticians have to face a number of choices, which results in a variety of models. A first distinction is made between the quasi-linear models, which are fast at the expenses of the accuracy, and non-linear models which are more accurate (they predict the existence of zonal flows and streamers) but are also more time consuming. The modeller has to choose also between the fluid approach and the gyrokinetic approach. The situation of the more commonly used available models is shown in Table 1 with regard to these possible options.

Because of the nonlinear nature of turbulence, the parametric dependences of the turbulent diffusive and convective flux terms cannot be determined completely analytically. However, analytical turbulent flux expressions can be used to determine 'local' dependences of the various coefficients (diffusion, thermodiffusion, curvature) around a situation of interest, by varying individually each of the parameters involved in the problem: impurity charge, $\nabla n_D/n_D$, $\nabla T_i/T_i$, etc. Note that in order to obtain analytical expressions (see below) one has to use a quasi-linear fluid model. These models do not have the ability of providing quantitative predictions of the diffusion coefficient, i.e. of the absolute particle flux. These can be obtained from nonlinear gyrokinetic models as was done in [?], with the limitation that only the flux is predicted, and not its diffusive and convective terms. In order to study the parametric dependences with this type of models, one can use the same method as above but it does not allow to separate the various flux terms. Moreover, the computing time necessary to cover the range of parameters explored by present day experiments or the range of predicted pramaeters of ITER makes this method unusable with the computers available today worldwide.

All these models can be used with fixed gradients, i.e. with a given background plasma from which the model deduce the turbulence characteristics. This is useful when an experiment is to be analysed. The limitation of this approach is that the model may need unrealistic sources of particles or energy to maintain the input gradients. An alternative approach, available in TRB, is to impose the fluxes, i.e. the sources (which can be determined experimentally or calculated), and evolve the profiles (i.e. the gradients) until a stationary state is reached. This method is useful to study for example the parametric dependences but may be unsuitable in some cases since the resulting state is not constrained and can be different from the experimental observations.

Some of these models (like GS2) retain only the eigenvalue corresponding to the most unstable mode whereas others (KINEZERO) have the ability to follow all the unstable modes. As there can be substantial differences in the predictions made by these two methods, for example in the direction of the convective flux direction, it is important to specify which method is used.

Finally, it is remarkable that most of the available models have been written originally for background plasma transport studies. In general they include a single impurity species which contributes to the total turbulence but the turbulent impurity flux is not always available. In this respect two models investigate in more detail the impurity case: TRB which has the ability to predict the turbulent transport coefficients for a single impurity species, and EDWM which treats the realistic case of an impurity species with any number of ionisation stages.

3.2 TURBULENT FLUX EXPRESSION

Quasi-linear calculations of the turbulent flux of an impurity has been performed in several publications [20, 21]. The quasilinear calculations consist of two steps. First, the evolution equations are linearized to calculate the response of the impurity population to a background turbulence. The underlying assumption is that the relative fluctuations are small enough that the nonlinear terms can be neglected. Second, a choice of the turbulence spectrum is made to obtain the impurity flux. This choice is critical as it affects significantly the calculated flux. If the impurity concentration is low enough, it does not influence the turbulence spectrum: the impurity behaves as a trace. It can be shown that in this case, the impurity flux can be expressed as the sum of a diffusive term and a convective term, similarly to the neoclassical flux:

$$\Gamma_Z = -D_Z^{turb}\,\nabla n_Z + \nu_Z^{turb} nZ \tag{14}$$

where the diffusion coefficient D_Z^{turb} and the pinch velocity ν_Z^{turb} do not depend on the impurity properties but only on the background plasma turbulence. However, the parameter domain in which the impurity does not influence the plasma and the nonlinearities can be neglected in the density response has not been studied in detail. In particular it is not known whether it is the case for the ITER case defined above.

Some analytical insight in the transport properties can be gathered without specifying any specific turbulence spectrum. Indeed, three mechanisms leading to an impurity convective flux have been investigated:

- a “curvature pinch” [20] which is always inward, and independent of the charge or mass of the considered species;
- a “thermodiffusion pinch” [20] which is inward for dominant electron turbulent modes, and outward for dominant ion modes.
- and a “parallel velocity pinch” [21], outward for dominant electron modes and inward for dominant ion modes.

These quasilinear fluid results have been confirmed by quasilinear gyrokinetic calculations with GS2 [21] and by nonlinear fluid calculations with the TRB code [22], which calculates a $\nu_Z^{turb} / D_Z^{turb}$. Only nonlinear gyrokinetic calculations would allow quantitative assessment of the various terms above.

Depending on the plasma conditions, the turbulence effects are dominantly carried by ions (ion temperature gradient (ITG) modes) or electrons (trapped electron modes (TEM) or electron temperature gradient (ETG) modes). The turbulence spectrum measurements indicate that in most situations ETG modes, characterised by large wavenumbers, have a weak contribution to the global turbulence. The destabilisation of TEM and ITG modes is driven in particular by the density and temperature gradients as shown on Fig.3. As can be seen, the ($\nabla n/n, \nabla T/T$) space is divided in four regions: at low normalised density and temperature gradients (or large gradient lengths) both types of modes are stable and turbulence is weak. At higher temperature gradients the ITG modes are destabilised while at higher density gradients the TEM are destabilised. If both gradients are strong, both types of modes will contribute to turbulence. Accurate and quantitative predictions of the stability thresholds cannot be obtained by the fluid models used to provide this qualitative result. Moreover, other parameters like the T_i/T_e ratio determine the stability thresholds. As an example the effect of the effective charge of the plasma (Z_{eff}) has been studied with a linear stability analysis performed with KINEZERO. The global stabilising effect of increasing the Zeff on the growth rates is illustrated on Fig.4 [18] for a radiative improved (RI) mode plasma in TEXTOR [25]. It had been previously reported in [23]. The main physical reason for this effect is that impurity seeding at a given electron density is accompanied by dilution. As a consequence the total ion pressure gradient, and thus the interchange drive, are decreased. This explanation is consistent with the results reported in [34]. An exception to this general effect is that increasing Z_{eff} can be destabilising for a at density profile close to the stability threshold, as already shown in [24] and as illustrated on Fig.3 for ITG-TEM thresholds claculated by KINEZERO. In ITER, assuming a moderately peaked density profile, the stabilising effect through dilution is expected to be the dominant mechanism.

The physical hypothesis behind the quasi-linear developments is that the studied impurity does not contribute the total turbulence, i.e. the trace-impurity situation. The validity domain of this hypothesis has not been studied in detail and so it is not known whether it is valid for ITER predictions. It should be kept in mind that, despite the simple quasi-linear expression and contrary to the neoclassical flux, the turbulent flux is not linear. By this we mean for instance that the $\nabla T_i/T_i$ and $\nabla n_D/n_D$ dependences are also contained in the diffusion coefficient and other terms.

The influence of electromagnetic effects on the turbulent impurity transport have not been studied extensively yet. The control parameter for these effects is β, the ratio of kinetic pressure to magnetic pressure : high β means a high energy content available for magnetic perturbations and low static magnetic field - this allows high relative magnetic field perturbations. However, most β-scaling experiments to date have been focused on heat confinement and overlooked particle and impurity transport. The observed dependence on β is weak; this indicates a mainly electrostatic turbulence and is a hint of a β independent impurity transport.

4. THE MAIN PARAMETRIC DEPENDENCES

4.1 PARAMETRIC DEPENDENCE OF D_{turb}/D_{neo}

4.1.1 Theoretical predictions

Quantitative neoclassical predictions have been available for a long time thanks essentially to the linear nature of the theory. As far as the turbulence theory is concerned, its non-linearity has long been an obstacle. Even today, few theoretical models (namely the non-linear gyrokinetic models) are in principle able to predict absolute diffusion coefficients. It is thus difficult to predict which phenomenon will dominate transport in a given situation. However a statement can be made about the neoclassical coefficients: it can be seen in all the examples given in the present publication that the diffusion coefficient is always in the range $10^{-3} \leq D_{neo} \leq 10^{-1} m^2/s$. This can be considered as a general result and is actually straightforward given the analytic expression of the coefficient. The v/D ratio can also be seen from expressions (4), (7) and (12) to be bound by the extreme situations where either of $\nabla n_D/n_D$ or $\nabla T_i/T_i$ is 0, which gives the approximate bounds:

$$\left| \alpha \frac{\nu_{n}eo}{D_{n}eo} \right| \leq Z \tag{15}$$

Conversely, assuming the anomalous experimental transport coefficients are due to turbulence, one notices that their values vary on a much wider range, from less than the neoclassical predictions up to a few m^2/s. The nature of impurity transport is thus determined essentially by the turbulence level.

4.1.2 Experimental situations

Experimental studies of impurity transport have explored most of the confinement regimes developed in the various tokamaks for the last twenty years. Let us sort these confinement regimes in four broad categories: ohmic, L-mode (with auxiliary heating and energy confinement time τ_E less than or equal to the ohmic scaling), H-mode (the enhanced τ_E is related to an edge transport barrier) and inner transport barrier (ITB) (the enhanced τ_E is related to a transport barrier located in the core plasma). Some of the published results concern mixt regimes such as the quiescent double barrier (QDB) regime on DIII-D in which two transport barriers develop.

In ohmic and L mode most publications report consistently a central region where the diffusion coefficient is either moderately anomalous like in Tore Supra [26, 27] and in JET [28, 30] or neoclassical like in CDX-U [31] and TCV [32]. Note that the Tore Supra and JET results concern the quiescent phase between sawteeth. In TCV, the convection velocity in the same region is neoclassical whereas in CDX-U it is a factor of about 2 below the neoclassical predictions.

In H mode, the observed transport is anomalous with variations from one result to another. In JET [29], similarly to the ohmic and L-mode results, the diffusion coefficient in the central region of the plasma is consistent with the neoclassical prediction. No difference between ICRF-heated and NBI heated H-mode plasmas is reported. In Alcator C-Mod H-mode plasmas heated by ICRH [42], the diffusion coefficient, although reduced compared to the L-mode case, is strongly anomalous over the whole plasma. In ASDEX-U [11], when the effect of the centrifugal force is taken into account for the heavier two species, both diffusion and convection of Ne, Ar, Kr and Xe are found close to neoclassical in H-mode plasmas heated by neutral beam injection only. The role of the heating scheme used to trigger and sustain the H mode in JET has been demonstrated in [33] and will be discussed later in this paper.

Various ITB scenarios have been developed since the late ‘90s (descriptions and characteristics of these scenarios can be found in the publications cited in this paragraph and their bibliography) with the benefit of high electron and/or ion pressure in the plasma core, i.e. better confinement. This improvement is generally attributed to a weaker turbulence level. The corollary is that the observed main species transport is closer to the neoclassical predictions than in other confinement regimes. Several studies have been dedicated to impurities with the same qualitative result but a number of questions. In TFTR [44] the diffusion coefficient for T, He and C has been found close to neoclassical whereas the comparison of the observed convection velocity with its neoclassical calculation is not considered conclusive due to experimental uncertainties. In the DIII-D quiescent double barrier regime [47, 57] the dffusion coefficients of He, N and Ne are larger than neoclassical. The convection velocity is also anomalous except maybe close to the magnetic axis, where anyway the validity of the neoclassical theory is questionable because of the large banana orbit widths. The authors mention that in this regime turbulence is not completely suppressed, which could be the reason for the anomaly. In JET the diffusion coefficients of Ne and Ni are found neoclassical. The neon convection velocity is neoclassical but that of nickel departs from its neoclassical calculation [60]. In FTU neither diffusion nor convection are found neoclassical [61].

As can be seen the comparison between observed and neoclassical transport vary from one experiment to another more than could be expected from the experimental uncertainties. It should also be noticed that even in cases where either of the transport coefficient is anomalous (a fortiori if both are) accumulation (in the sense of a higher impurity density profile peaking than the ion peaking) can occur. Conversely, a neoclassical situation does not always lead to central peaking of the impurity density profiles, due to the temperature screening effect describes above. The global experimental picture of impurity transport in ITB scenarios is thus confused and needs to be reworked in order to provide information about theories. In particular concerning the relation between the observed transport and the measured turbulence characteristics, the published literature is very sparse and only qualitative. For example in Refs. [47] and [62], impurity transport and turbulence observations are studied separately, the anomalous diffusion being explained by a heuristic turbulence model.

4.2 CONVECTIVE FLUX

4.2.1 Theory

As has been seen earlier, the direction of the neoclassical convective flux for a given impurity depends on its charge and on the plasma conditions. Calculations in as different situations as possible (charge, collisionality, background plasma density and temperature) show that the thermodiffusion term of the Pfirsch-Schlüter flux is directed outward in most cases (see for instance [11]. The banana-plateau thermodiffusive term can be in either direction. In other words, for an impurity which is fairly deep in the Pfirsch-Schlüter collisional regime, the direction of the convective flux is essentially determined by the ratio of the main ion density to temperature gradients: if this ratio is larger than 1/2, the convective flux is inward, almost independently of the impurity mass and charge (of course the heavy, highly charged impurities are more likely to be in this regime). For an impurity which has a banana-plateau flux comparable to or higher than the Pfirsch-Schlüter flux, the thermodiffusion part of the convective flux is almost always inward and thus enhances the peaking due to the main ion density gradient term.

Turbulent convection has been investigated with two approaches. The nonlinear gyrokinetic approach has been followed in [63] using the GYRO code. The case of a deuterium plasma with He as the single impurity is studied, including the potential contribution of the impurity to the total turbulence (i.e. the trace hypothesis is not made). The authors investigate the parametric dependence of the convective flux on the normalised He density gradient $\nabla n_{He}/n_{He}$ and on the He concentration c_{He} (Fig.5). For negative $\nabla n_{He}/n_{He}$ and $\nabla n_D/n_D$ (peaked ion density profiles) the He convective flux is outward if $|\nabla n_{He}/n_{He}| \leq 1.4|\nabla n_D/n_D|$, i.e. if the He density profile is not much more peaked than the deuterium one, and outward otherwise. In other words, since these simulations are made with a fixed gradient code, the steady state is reached when $n_{He} \propto n^{1.4}_D$, resembling the neoclassical result $n_{He} \propto n^2_D$. It is inferred from the investigated values of c_{He} (0.5% and 1.5%) that this result does not depend on the He concentration. A quasilinear kinetic model is used to interpret the He convection dependence on $\nabla nH_e/nH_e$ as a curvature effect. Note that in this simple model the parallel dynamics is not taken into account.

The case of a plasma with an unspecified main ion species and a single impurity species present as a trace is studied with a quasilinear fluid approach [21]. In addition to the $\vec{E} \times \vec{B}$ advection term, identical for all species, the term related to the parallel compression effect is shown to be outward for electron modes, inward for ion modes. The term proportional to $\nabla T_i/T_i$, analogous to the thermodiffusion term for electron transport, is found to be in the opposite direction: outward if turbulence is dominated by ion modes and inward if it is dominated by electron modes. It is always smaller than the parallel compression term. The quasilinear predictions of the curvature convective flux are in agreement with experimental results with ion and/or electron heating (see below).

A linear calculation with KINEZERO shows that the dominant modes in the ITER reference case, i.e. with a at density profile, are ITG modes which drive an outward thermodiffusion ion and impurity flux (Fig.6). The same calculation predicts an inward curvature-compressibility flux independently of the impurity mass and charge. The latter flux is higher and determines the direction of the total turbulent convective flux.

4.2.2 Experiment

Comprehensive and detailed studies of the convective flux parametric dependences are difficult due to at least two reasons:

i) Many of the involved parameters (n_D, T_i, T_e, ∇n_D, ∇T_i, ∇T_e, q, n_Z, m_Z, Z, . . .) are linked to each other in the experiments. For instance the electron and ion temperatures, and thus their gradients, are generally closely coupled by the energy equipartition. It is thus difficult to evidence their opposite roles on the dominant turbulent modes, and hence on the convective flux direction.

ii) As emphasised above, there are very few situations in which neoclassical transport has been found dominant, hence the difficulty of evidencing its experimental dependences. More generally, it is very rare that one can design and realise an experiment in which either of these phenomena, collisions or turbulence, is known a priori to be dominant.

An additional reason, which can be overcome, is that most of the particular regimes in which there are chances of observing a pure transport phenomenon are not predictable enough to allow impurity transport studies. When such regimes as ITB regimes are better controlled, it can be expected that impurity transport will become a high priority programme.

Notwithstanding these difficulties, a number of experimental confirmations of the theoretical predictions have been given. As for the neoclassical theory, the main concern has been impurity accumulation in the plasma core [38, 11, 46]. Note however that in TFTR, the persistent hollow tritium density profile is attributed to the low, neoclassical diffusion coefficient in the plasma core [43]. In general the studies are limited to a semi-quantitative comparison of the experimental results with neoclassical calculations. The convective flux dependence on the ion temperature gradient is studied in more detail in two publications. The DIII-D experimental situation of the so-called VH mode [47] is noticed to feature the pre-requisite of neoclassical convection tests: low turbulence, at density profile and strong ion temperature gradient. The results, from which the residual turbulence effects are subtracted using a heuristic model, are consistent with the theoretical predictions. The other detailed experimental study [49], performed in Alcator C-mod, explains the impurity penetration across the edge pedestal by the inward convective flux due to the neoclassical-like ion density gradient dependence in this region.

Anomalous convection has been found in many experiments (see e.g. [27] in which the sawtooth effect is isolated from the main transport effects, [51] which describes an anomalous pinch leading to impurity accumulation), some of the most recent ones using various heating schemes to show striking evidence of the predicted turbulent effects. In ASDEX-U improved H-mode plasmas, central ECRH is routinely used to prevent tungsten accumulation in the plasma centre [52]. A detailed study [53] of the heating scheme (NBI only or NBI with RF scheme, deposition radius) effect on silicon transport shows that, in the central region (where transport is neoclassical with NBI only), ECCD in the counter-current direction enhances the central diffusion coefficient and induces an outward contribution to the convective flux. This effect is more marked when the plasma current is decreased from 1 MA (q_{95} = 3.8) to 0.8MA (q_{95} = 4.9–5.3). In H-mode plasmas with pure ICRH absorbed predominantly by electrons, the diffusion coefficient in the plasma centre is neoclassical and the convective flux is inward for off-axis power deposition. For on-axis deposition, the central D is anomalous and v vanishes. Although the authors do not compare the experimental results with turbulent predictions, we note that they are consistent with TEM destabilised by the stronger electron temperature gradient and driving an outward convective flux due to parallel compression.

The same type of experiment has been performed at JET and compared with quasilinear gyrokinetic calculations performed with GS2 [65]. Ni transport has been studied in plasmas heated with ICRH either in ^{3}He minority heating scheme or in ^{3}He mode conversion scheme. In the first type of discharges, the central diffusion coefficient is close to neoclassical and the convection velocity is inward. In the second type, the central diffusion is higher and the convection velocity is slightly outward or zero (Fig.7). The data analysis provides two possible explanations: the different heating channels (ions in minority heating scheme, electrons in mode conversion) or the different power deposition radii (r/a = 0.1 and r/a = 0.37 respectively). A quasilinear analysis of the ITG modes and TEMs in these plasmas points out the contribution of the convective term due to parallel velocity compression. As described in [21] and summarised in §4.2.1, this term is strongly outward in the case of highly negative normalised electron temperature gradient which corresponds indeed to the experimental situation of the mode conversion discharges.

4.3 IMPURITY CHARGE DEPENDENCE

4.3.1 Theory

The central electron temperature of an ITER H-mode plasma is expected to be about 20 keV. At this temperature the impurity with the highest charge would be W^{62+}. With T becoming a routinely injected species in ITER, the wide impurity charge range gives incentive to study the predicted Z dependence of all flux terms described above.

In order to make the phenomenon clearer we will start by fixing the impurity mass (to 184) and varying only the charge (from 2 to 74).

As can be seen from the approximate expressions 3, 6, 11 and Fig. 8, the classical and Pfirsch-Schlüter diffusion coefficients do not depend on Z. This remains true as long as the main ion collisionality is low. As the banana-plateau diffusion coefficient decreases with increasing Z, the total coefficient decreases too although the impurity collisionality increases. Going to higher impurity collisionality regions, D approaches its asymptotic value for lower Z due to the higher relative contribution of the Pfirsch-Schlüter term. Note also that the asymptotic coefficient increases with r/a due to the q dependence of D_{PS} but never gets higher than 10^{-2} m^2/s. In experimental situations, in order to increase Z in a given plasma region, one has to increase also the mass. Moreover, in order to keep the impurity at the trace level, one has to reduce the number of injected particles (hence the impurity concentration) as Z and m_Z are increased. The m_Z and c_Z effects on the diffusion coefficient are very weak and do not change the general picture given above: for light impurities (He, Be, C, Ne) near the plasma centre, D_{neo} can be more than one order of magnitude higher than for heavy impurities (W). Further from the centre, this factor is about 4 as shown in [66].

The strength of the temperature screening effect, quantified by the ratio $-\alpha_T/\alpha_n$ (see §2.1), is shown on Fig.9 as a function of the impurity. The effect of c_Z is still weak but it can be seen for Fe and Ni, for which an arbitrary concentration of 5×10^{-5} has been assumed (Fe and Ni are not intrinsic impurities ITER, nor are they planned for particular scenarios). The screening strength increases with Z from 0.2 for light species like He or Be to about 0.5 for heavy species. This means that to balance the $\nabla n_D/n_D$ convective term, the ion temperature gradient will have to be much stronger for light impurities: the neoclassical convective flux is outward if $L_T/L_n > 5$ for He, if $L_T/L_n > 2$ for W. It is thus possible, in principle, to observe convective fluxes in opposite directions for different impurities: inward for light impurities, outward for heavy impurities. Note also that the outward convective flux condition above will be automatically realised if the density profile is at, for example in the case of neoclassical main ion transport and plasma current entirely sustained by non-inductive means. The existence of an anomalous inward particle pinch in several experiments makes this expectation debatable but the use of additional power schemes as summarised above could provide such a situation and thus help prevent any impurity accumulation. Finally, Ref [66] shows the neoclassical convection velocities calculated by the code NEOART in an ITER FDR case, taking into account the effect of collisions between different impurity species. Although the existence of non-zero gradients gives a more complex shape to the radial profiles of the convection velocity, the qualitative result above remains unchanged.

Lastly, the impurity charge plays a role not only in the convection direction but also in the absolute value of the convection velocity: $v_Z \propto ZD_Z$. With D_Z decreasing toward an asymptotic value when Z is increased, as shown in the previous paragraph, it can be expected that in general the convective effects will be more easily observed by studying very light or very heavy impurities.

The Z dependence of the turbulent diffusion coefficient is explicited in [21]. The first term in D^{turb}_Z, corresponding to the random walk of every particle about the fluctuating potential with the $\vec{E} \times \vec{B}$ drift velocity $\tilde{\vec{v}}_{\vec{E}\times\vec{B}} = -\nabla\tilde{\phi} \times \vec{B}/B^2$, independent of the particle charge. The other terms are decreasing functions of Z so that, as for neoclassical diffusion, D^{turb}_Z is predicted to tend to an asyptotic value at high Z.

The dominant term in the convection velocity, due to parallel velocity compression, is proportional to the charge to mass ratio Z/A, which is almost independent of Z. This term thus remains finite even at high Z. Note also that no Z dependence of the sign of this term is reported, which means that the corresponding flux direction is predicted to be the same for all trace impurity species. The thermodiffusion term (the term proportional to $\nabla T_i/T_i$) scales roughly as 1/Z but, although weak compared to the parallel compression term, does not vanish until $Z > 100$, well above the maximum expected impurity charge even in the ITER plasmas. The convection velocity comprises also an $\vec{E} \times \vec{B}$ compression term, small but independent of Z. At high Z, v^{turb}_Z thus tends asymptotically to the sum of this term and of the parallel compression term, the latter being determined by the dominant turbulent modes, ITG or TEM.

The theoretical Z dependences of the transport coefficients are summarised on Table 2.

4.3.2 Experiment

In present day tokamaks the range of common intrinsic impurities is somewhat narrower than predicted in ITER but it allows to test the theoretical Z dependence. It spans from helium (A = 4,Z = 2) to nickel (A = 59,Z = 28) with a few tokamaks dealing with heavier species such as molybdenum (A = 96,Z = 42) in FTU and tungsten (A = 184,Z = 74) in ASDEX-U. Due to the maximum electron temperature the heaviest species are not completely stripped and thus the intrinsic impurity charge cannot be much higher than 46 (W at T_e = 3.5 keV in the centre of an H-mode plasma in ASDEX-U). For a given set of plasma parameters, increasing the impurity charge can be done only by using heavier and heavier species, which leads to a Z/A ratio decreasing very slowly from 1/2 for helium to 1/3 for W in the centre of the ITER reference pasma (1/4 in the centre of an ASDEX-U H-mode plasma).

SYNTHESIS AND CONCLUSIONS

Approximate flux expressions of the collisional transport have been used to explicit the parametric dependences of neoclassical transport. The coefficients are shown to depend weakly on the main ion collisionality in the present day tokamaks and in ITER. The diffusion coefficient decreases with increasing impurity charge, due only to the banana-plateau term. The convection velocity, both in sign and in absolute value, depends on the ratio of the ion temperature to density gradient lengths and on the impurity charge. For the most common situations where both gradients are negative (peaked profiles), the so-called temperature screening effect is always effective.

In order to enhance its effectiveness, one could decrease the ion temperature gradient length. However there is a risk of destabilising the ion turbulent modes (see below). The temperature screening strength increases with Z, which is rather favourable to global plasma performances because heavy impurities radiate more than the light ones in the plasma core and because efficient heating requires taht the He lifetime be longer than that of other impurities. No systematic test experiments of these dependences were performed. Few publications report on exclusively neoclassical transport but when it is so, the results are consistent with the predictions. Theoretical models for turbulent impurity transport have exploited several available paths (quasilinear and nonlinear, fluid and gyrokinetic, fixed gradients and fixed fluxes,...). They converge toward predictions concerning the effect of the dominant turbulent modes on the convective flux (inward for dominant ion modes, outward for dominant electron modes). This could be in conflict with attempts of improving the neoclassical temperature screening by strengthening the ion temperature gradient. The diffusion coefficient is predicted to be an asymptotically decreasing function of Z, the dominant terms of the convection velocity are essentially independent of Z. Quantitative predictions are scarce due to the need for nonlinear gyrokinetic calculations, which are time demanding. Recent experiments have confirmed qualitatively the turbulent convection predictions.

REFERENCES

[1]. J.W. Connor, Plasma Phys. Vol. **15** (1973) 765.

[2]. F.L. Hinton, T.B. Moore, Nucl. Fusion Vol. **14** (1974) 639.

[3]. A. Samain, EUR-CEA 745 report (1974).

[4]. P.H. Rutherford, Phys. Fluids Vol. **17** (1974) 1782.

[5]. S.P. Hirshman, Phys. Fluids Vol. **19** (1976) 155.

[6]. S.P. Hirshman, PPPL-1291 report (1976).

[7]. S.P. Hirshman, D.J. Sigmar, Nucl. Fusion Vol. **21** (1981) 1079.

[8]. K.W. Wenzel, D.J. Sigmar, Nucl. Fusion Vol. **30** (1990) 1117.

[9]. Y.B. Kim et al., Phys. Fluids B Vol. **3** (1991) 2050.

[10]. W.A. Houlberg et al., Phys. Plasmas Vol. **4** (1997) 3230.

[11]. R. Dux et al., Nucl. Fusion, Vol. **39** (1999) 1509.

[12]. K.D. Zastrow et al., Plasma Phys. Control. Fusion, Vol. **46** (2004) B255.

[13]. J. Rapp et al., Plasma Phys. Control. Fusion, Vol. **39** (1997) 1615.

[14]. H. Nordman et al., Nucl. Fusion, Vol. **30** (1990) 983.

[15]. R.E. Waltz et al., Phys. Plasmas, Vol. **4** (1997) 2482.

[16]. X. Garbet & R.E. Waltz, Phys. Plasmas , Vol. **3**(1996) 1898.

[17]. M. Kotschenreuther et al., Phys. Plasmas, Vol. (1995) 2381.

[18]. C. Bourdelle et al., Nucl. Fusion, Vol. **42** (2002) 892.

[19]. J. Candy et al., Phys. Rev. Letters ,Vol. **03** (2003) 045001.

[20]. X. Garbet et al., Phys. Plasmas Vol. **12** (2005) 082511.

[21]. C. Angioni et al., Phys. Rev. Letters, Vol. **96** (2006) 095003.

[22]. N. Dubuit et al., submitted to Phys. Plasmas.

[23]. R.R. Dominguez et al., Nucl. Fusion, Vol. **29** (1989) 84.

[24]. R. Paccagnella et al., Nucl. Fusion, Vol. **30** (1990) 545.

[25]. U. Samm et al., Plasma Phys. Control. Fusion, Vol. **35** (1993) B167.

[26]. M. Mattioli et al., Nucl. Fusion, Vol. **38** (1998) 189.

[27]. M. Mattioli et al., Nucl. Fusion, Vol. **38** (1998) 1629.

[28]. D. Pasini et al., Nucl. Fusion, Vol. **30** (1990) 2049.

[29]. D. Pasini et al., Plasma Phys. Control. Fusion, Vol. **34** (1992) 677.

[30]. R. Giannella et al., Nucl. Fusion, Vol. **34** (1994) 1185.

[31]. V.A. Soukhanovskii et al., Plasma Phys. Control. Fusion, Vol. **44** (2002) 2339.

[32]. E. Scavino et al., Plasma Phys. Control. Fusion, Vol. **45** (2003) 1961.

[33]. L. Garzotti et al., 10th EU-US Transport Task Force Meeting, Varenna, 2004.

[34]. M.Z. Tokar' et al., Phys. Rev. Letters ,Vol. **84** (2000) 895.

[35]. G.T. Hoang et al., Phys. Rev. Letters ,Vol. **90** (2003) 155002.

[36]. H. Weisen et al., Europhys. Lett. **56** (2003) 542.

[37]. D.R. Baker et al., Nucl. Fusion Vol. **40** (2000) 1003.

[38]. K. Ida et al., Phys. Rev. Letters ,Vol. **58** (1987) 116.
[39]. R. Giannella et al., 16d EPS Conference on Control. Fusion and Plasma Phys., 1989, Venice.
[40]. M.R. Wade et al., Phys. Plasmas, Vol. **2** (1995) 2357.
[41]. M. von Hellermann et al., 22d EPS Conference on Control. Fusion and Plasma Phys., 1995, Bournemouth.
[42]. J.E. Rice et al., Phys. Plasmas, Vol. **4** (1997) 1605.
[43]. P.C. Efthimion et al., Phys. Plasmas, Vol. **5** (1998) 1832.
[44]. P.C. Efthimion et al., Nucl. Fusion, Vol. **39** (1999) 1905.
[45]. K.-D. Zastrow et al., 26d EPS Conference on Control. Fusion and Plasma Phys., 1999, Maastricht.
[46]. H. Chen et al., Phys. Plasmas, Vol. **7** (2000) 4567.
[47]. M.R. Wade et al., Phys. Rev. Letters, Vol. **84** (2000) 282.
[48]. J.E. Rice et al., Phys. Plasmas, Vol. **7** (2000) 1825.
[49]. T. Sunn-Pedersen et al., Nucl. Fusion, Vol. **40** (2000) 1795.
[50]. M. Mattioli et al., Nucl. Fusion, Vol. **38** (1998) 1629.
[51]. E. Scavino et al., Plasma Phys. Control. Fusion, Vol. **46** (2004) 857.
[52]. R. Neu et al., Plasma Phys. Control. Fusion, Vol. **44** (2002) 811.
[53]. R. Dux et al., Plasma Phys. Control. Fusion, Vol. **45** (2003) 1815.
[54]. H. Chen et al., Nucl. Fusion, Vol. **41** (2001) 31.
[55]. J.E. Rice et al., Nucl. Fusion, Vol. **41** (2001) 277.
[56]. C. Giroud et al., 28th EPS Conference on Control. Fusion and Plasma Phys., 2001, Funchal.
[57]. W.P. West et al., Phys. Plasmas, Vol. **9** (2002) 1970.
[58]. V. Rohde et al., 19th IAEA Fusion Energy Conference, 2002, Lyon.
[59]. B. Zaniol et al., 30th EPS Conference on Control. Fusion and Plasma Phys., 2003, St. Petersburg.
[60]. R. Dux et al., Nucl. Fusion, Vol. **44** (2004) 260.
[61]. L. Carraro et al., Plasma Phys. Control. Fusion, Vol. **46** (2004) 389.
[62]. T.H. Osborne et al., Nucl. Fusion, Vol. **35** (1995) 23.
[63]. C. Estrada-Mila et al., Phys. Plasmas, Vol. **12** (2005) 022305.
[64]. C. Giroud et al., JET report EFDA-JET-CP(04)03-19, 2004.
[65]. M.-E. Puiatti et al., Phys. Plasmas, Vol. **13** (2006) 042501.
[66]. R. Dux et al., Nucl. Fusion, Vol. **40** (2000) 1721.

	Quasi-linear	*Non linear*
Fluid	*Weiland [14], GLF23 [15]*	*TRB [16]*
Gyrokinetic	*GS2 [17], KINEZERO [18]*	*GS2, GYRO [19]*

Table 1: Categories of turbulence models.

	Neoclassical	***Turbulence***
D_Z	*Decreasing function of Z* $\rightarrow D^{neo}{}_{asymp}$ *for* $Z > 30 - 60$	*Decreasing function of Z* $\rightarrow D^{neo}{}_{asymp}$
v_n	$ZD_Z \times \nabla n_D/n_D$ *Always inward*	
v_T	$ZD_Z\alpha_T \times \nabla T_i/T_i$ *In general* $\alpha_T < 0$, $\vert\alpha_T\vert$ *increases with Z*	*Decreasing function of Z* *outward Outward if ion modes dominant* *Inward if electron modes dominant* *Small term*
$v_{//comp}$		*Independent of Z* *Inward if ion modes dominant* *Outward if electron modes dominant* *Dominant term*

Table 2: Predicted impurity charge dependence of the transport coefficients.

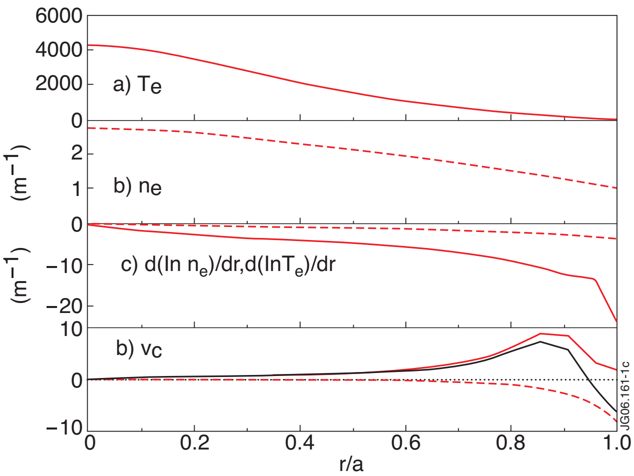

Figure 1: Radial profiles of the temperature (a), density (b), normalised temperature (dashed-dotted line) and density (dashed line) gradients (c) and of the convective velocities due to the main ion temperature and density gradients, and total (solid line) for fully non inductive discharge TS32299.

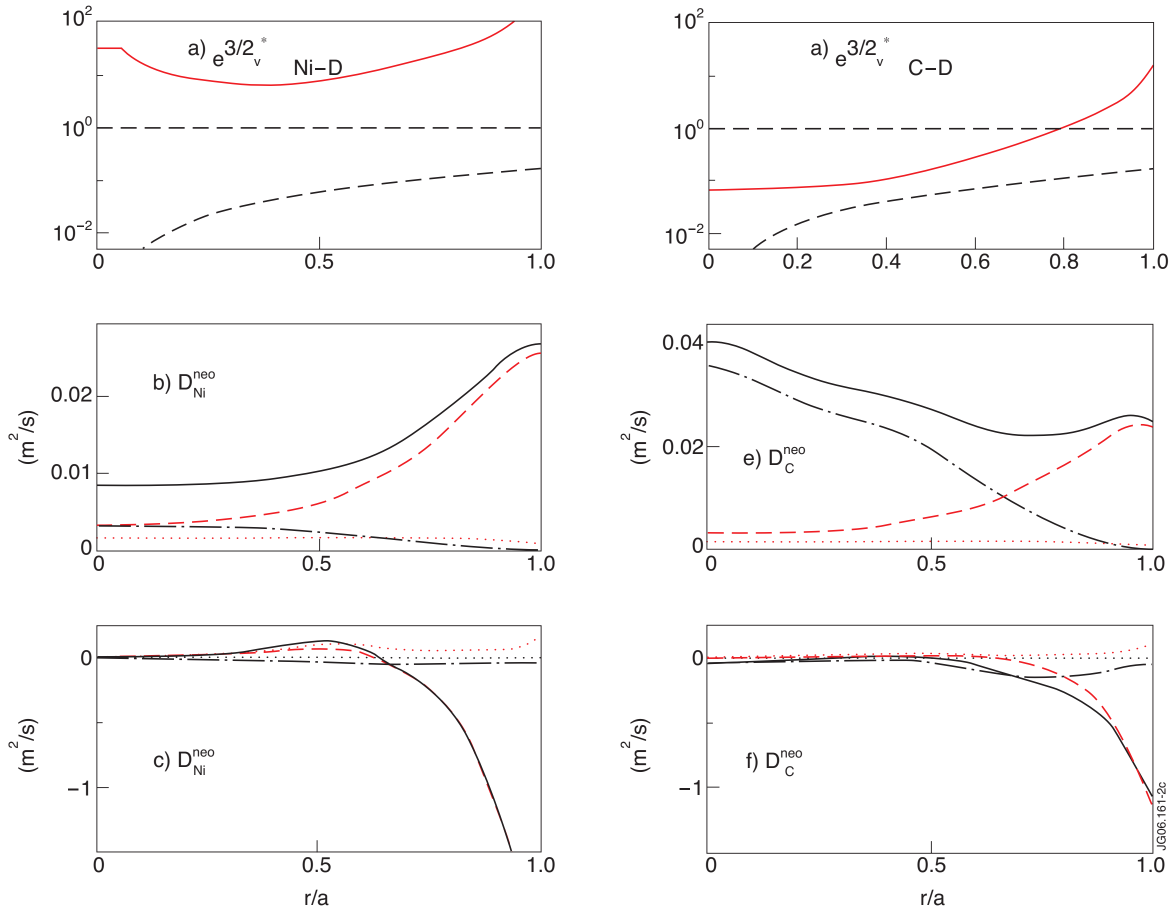

Figure 2: Radial profiles of the collisionality (a and d), neoclassical diffusion coefficient (b and e) and convection velocity (c and f) of injected nickel (left) and intrinsic carbon (right) for an ohmic Tore Supra discharge (TS35147). Solid line: total, dotted line: classical, dashed line: Pfirsch-Schlüter, dashed-dotted: banana plateau.

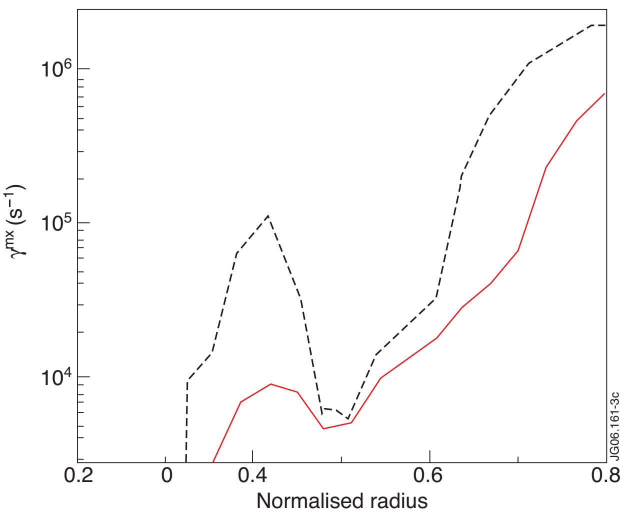

Figure 3: Radial profile of the maximum growth rate in an L-mode, Zeff = 1.2 discharge (68812, dashed line) and a RI-mode, Zeff = 2.7 discharge (68803, solid line) as calculated by KINEZERO.

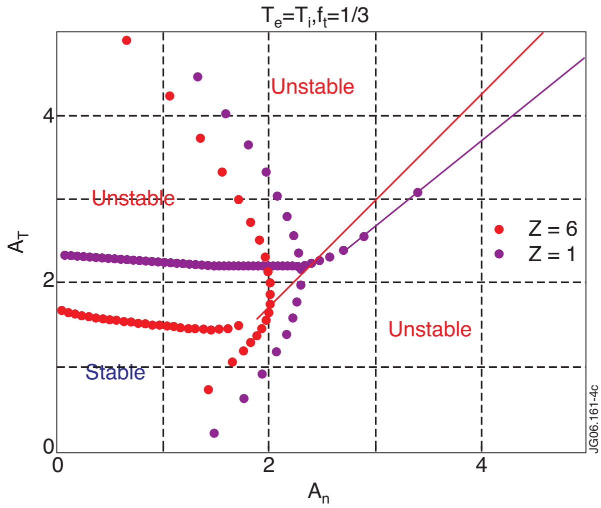

Figure 4: Stability regions of TEM and ITG modes as a function of the normalised density and temperature gradients as calculated by KINEZERO for $T_e = T_i$.

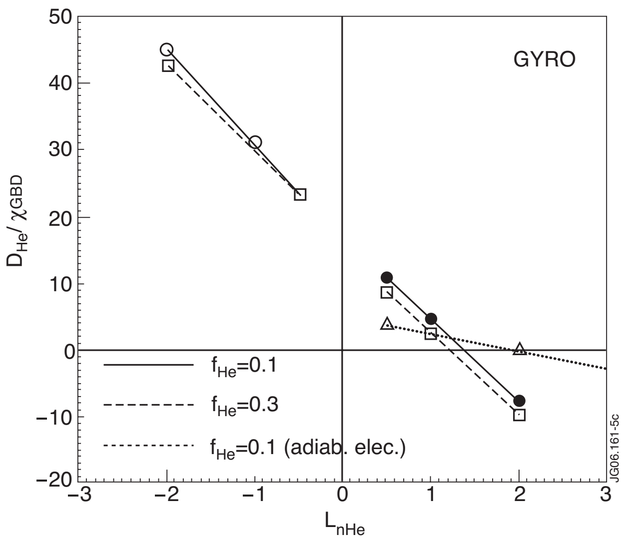

Figure 5: $\Gamma_{He}/\chi\nabla n_{He}$ as a function of the helium density gradient length.

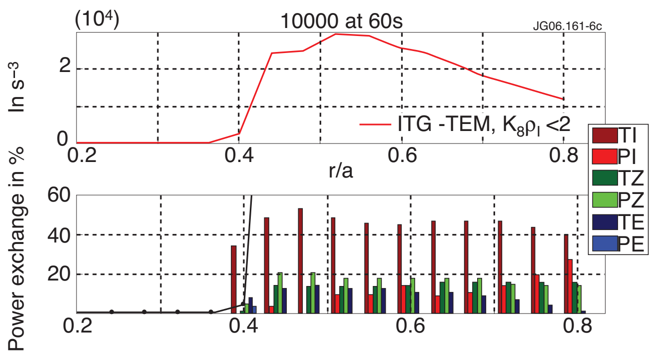

Figure 6: Dominant microturbulent modes in the ITER reference case.

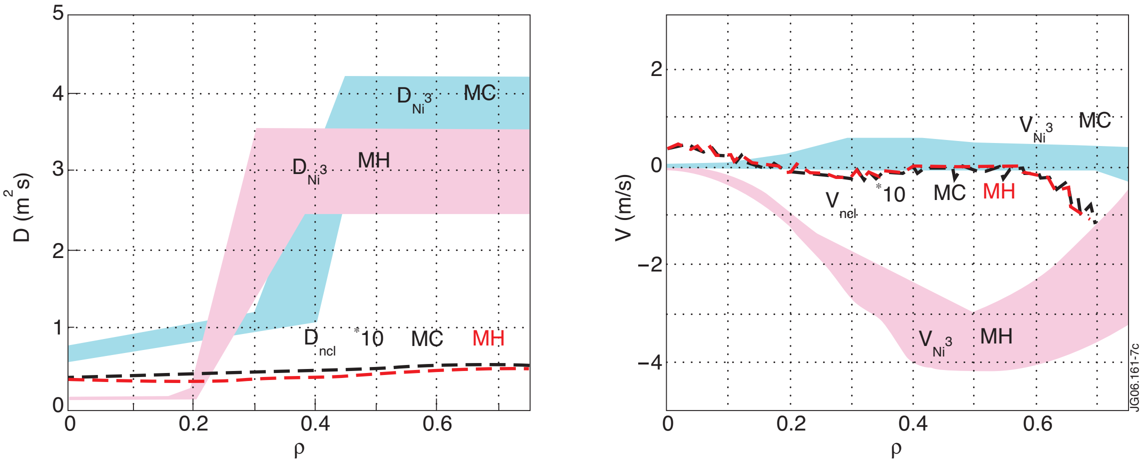

Figure 7: Observed nickel transport coe cients in ICRH minority heating (MH) and mode conversion (MC) schemes in JET H-mode plasmas.

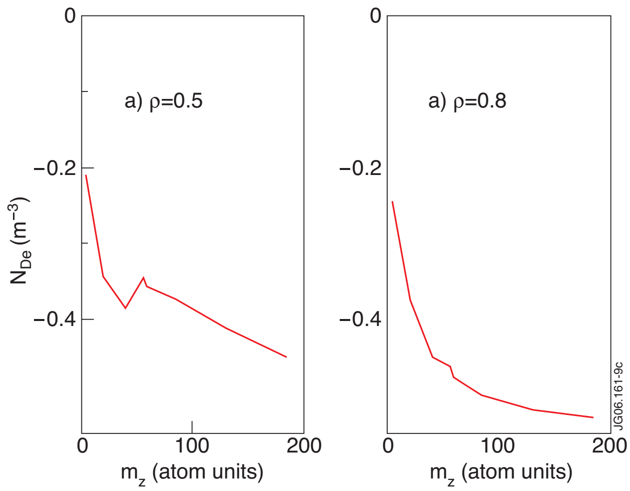

Figure 9: Neoclassical temperature screening strength dependence on the impurity species in the ITER reference case. a) at mid-radius, b) at ρ = 0.8.

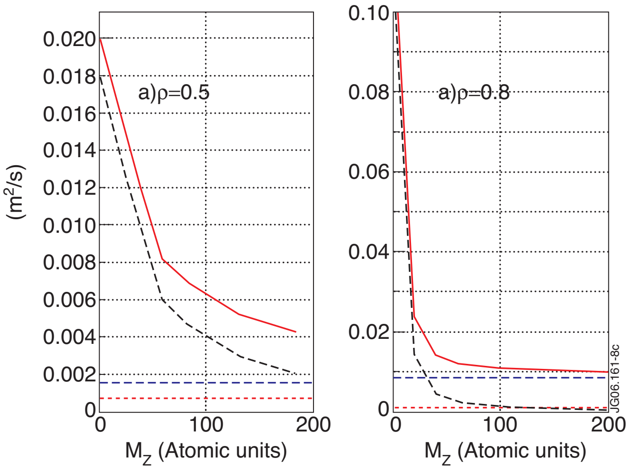

Figure 8: Neoclassical diffusion coefficient dependence on the impurity species.